Research Article

Flexural Toughening of Hooked-End Steel Fibers Reinforced Mortars

Giuseppe Gullì, Riccardo Bertino and Francesco Grungo
Tradimalt S.p.A., Via Nazionale 1, Villafranca Tirrena (ME), Italy

Davide Palamara, Paolo Bruzzaniti and Luigi Calabrese*
Department of Engineering, University of Messina, Contrada di Dio Sant'Agata, Messina, Italy

* Corresponding author. E-mail: lcalabrese@unime.it DOI: 10.14416/j.asep.2023.11.004
Received: 27 June 2023; Revised: 25 July 2023; Accepted: 18 August 2023; Published online: 14 November 2023

Abstract
This paper investigated the effect of hooked-end steel fiber at varying fiber content on the flexural toughening of fiber reinforced cement mortars (FRCM) by using three-point bending tests. In particular, to preserve the mortar workability, three low weight fractions (0.3%, 0.5% and 0.7%) and two cement matrices (M10 and M15) were investigated. The results showed that the mechanical bending behavior of the FRCM increases significantly at increasing fiber content and cement plaster matrix. An important aspect that has been addressed is how the flexural toughening is varied at varying fiber content and the type of matrix. Especially, all composite mortars exhibited a toughness index (TI) in the range of 10–45, indicating a suitable strengthening and toughening effect supplied by the hooked-end fiber addition. The best TI value, equal to 44, was experienced for the M10-D7 batch characterized by 0.7 wt.% of hooked-end steel fibers and an M10 cement matrix. Furthermore, unlike unreinforced concrete where brittle and unexpected failure occurs dominated by a sudden and catastrophic propagation of tensile cracks, the FRCM samples exhibited a ductile behavior with a marked residual post-crack resistance even for composites mortars with low metal fiber content.

Keywords: Cracking behavior, Flexural, Hooked-end fibers, Mortars, Toughness

1 Introduction

In the last years, fiber reinforced cementitious mortars (FRCM) have been widely explored in order to overcome the well-known weakness of cement-based materials under tensile stresses [1], [2]. The main goal of this approach is the potential improvement of the mechanical stability of the mortar providing a transition from a mainly brittle behavior toward a pseudo-ductile behavior [3]. In the engineering construction and maintenance field, a great design benefit can be potentially yield by addition of fibers to cement mortars in order to improve, toughness, compression and tensile strength [4]. If a suitable fiber-matrix interphase is ensured, the fiber reinforcements are able to retain the crack propagation [5] and offer a good stress transfer between the fibers and the cement matrix [6].

Several research activities were performed investigating the addition of different classes of materials as mortar reinforcement for advancement of construction technology and sustainable building practices [7]–[11]; Concerning short fibers different classes of materials are investigated, involving metal, ceramic, polymeric, synthetic fibers [12]–[15] or a combination of them [16]–[19]. In such a context, the incorporation of straight steel fibers is most promising considering its potential effectiveness in terms of ductility and energy absorption of the FRCM (up to 300 times higher than the unreinforced one) [20].

Kang *et al.*, [21] assessed the fiber distribution characteristics of the flexural strength of steel fiber-reinforced concrete. The results highlighted that the initial cracking strength and ultimate flexural strength of the FRCM placed parallel to the longitudinal direction

of the mold are 5.5% and 61% higher than the transversely placed ones. Rashad [22] also highlighted that the addition of steel fibers, although it has a negative effect on porosity and workability, it is beneficial for more mechanical-related performances (e.g. flexural strength, ductility, toughness, modulus of elasticity and of rupture). Yoo *et al.* [23], investigated the flexural behavior of ultra-high-performance concrete reinforced with hybrid straight steel fibers. Although the fiber bridging effect increases at increasing fiber length, the use of hybrid long/short fibers offers the triggering of detrimental negative contributions to toughness.

Compared with straight steel fiber, hooked-end steel fiber has potential to further improve mechanical properties and durability [24]. The role of hooked-end fibers is crucial in order to tailor the post-cracking performance as a consequence of fiber bridging of the crack section, thus providing both an effective crack stabilization effect and tensile strength improvement [25], [26]. Abushanab *et al.*, [27] observed that the pull-out and flexural strength of hooked-end steel FRCM is about 50% higher than the FRCM ones constituted by straight steel fibers. Analogous considerations were obtained by Wu *et al.*, [28] in terms of compressive strength and bending behavior of fiber reinforced ultra-high performance concrete. In particular, for concrete filled with 3% hooked-end fibers, the compressive strength increased by 48% compared to the concrete with the same amount of straight fiber incorporated. The positive effect of hooked-end steel fiber on post-cracking and residual flexural strength of concerted after aging, in high temperature treatment, was also assessed in [29], [30]. Besides, Fang *et al.*, [31] reported that hooked-end fibers and fibers with the highest aspect ratio reduce shrinkage more efficiently compared with straight fibers. Comparable observations can be acquired in [21], [32], wherein the significance of the hooked-end in ensuring dependable bond performance of steel fiber is emphasized. The appropriate length of hooked-end steel fiber can be optimized considering the bonding requirements. This approach offers a valuable means to quantitatively assess the suitability and applicability of steel fiber when utilized in concrete mortars.

Conversely, the impact of hook-ended steel fibers on workability compared to straight and corrugated ones significantly reduces the cement mortar slurry workability [33]. This last factor is fundamental for the applicability of the mortar, and it is therefore necessary to identify a composite mortar mix constituted by short steel fibers that favor its mixing and workability preserving the toughening and stiffening effect supplied by the fiber addition. Additional investigation is required to ascertain the actual impact of fiber distribution on the mechanical properties of concrete. In a previous study conducted by Kheddache *et al.* [34], the influence of steel fiber distribution on the bending behavior of self-compacting mortar was demonstrated. The research examined the effects of two types of steel fibers, straight and hooked, at varying low doses (20, 30, and 40 kg/m^3), on the flexural strength of the composite. Furthermore, the significance of this subject was further elaborated in another work [35], which investigated the effects of distributing low and high doses of hooked steel fibers on flexural strength. This confirms that the search for an in-depth analysis of reinforced mortars with low short fiber content is crucial to further investigate the applicability of these materials e.g. self-compacting, restoration, or retrofitting mortars.

The use of short metallic fibers, with a smooth waved end, represents a potentially effective approach to ensure adequate workability and drafting of the cementitious slurry, a fundamental parameter for example during the laying or mixing phase of the mortars. The identification of the optimal conditions for acquiring a tough mortar using these short steel fibers therefore is a possibly productive experimental strategy in this research context to obtain a mortar with high mechanical strength, toughness and adequate workability. As discussed above, these findings highlighted the relevant potential of this approach [24]. At the same time, an experimental approach proves fruitfully active in improving the knowledge of the mechanical behavior of fiber-reinforced cementitious materials and how this also affects their strength and fracture mode [29], [30]. Furthermore, in their study, Khan *et al.*, [36] explored the utilization of the magnetic field method as a technology for producing aligned hooked-end steel fiber cementitious composites, while evaluating its impact on the fracture behavior of the cementitious concrete. The findings revealed significant improvements, with the cracking load and ultimate load increasing by approximately 24–55% and 51–86%, respectively, depending on the

content of added fibers. However, there is still a need for additional research to enhance our understanding, particularly regarding the toughness and post-fracture resistance capacity of these novel Fiber-Reinforced Cementitious Mortars (FRCM). Conducting further studies in this area would prove valuable in gaining deeper insights into the behavior and performance of these materials when utilized in reinforced plasters.

By delving into the toughness of FRCM, researchers can investigate how these materials can withstand and absorb energy during deformation and crack propagation. Understanding the post-fracture resistance capacity is equally crucial, as it sheds light on the ability of FRCM to maintain structural integrity and carry load even after experiencing a fracture. The correlation of the post-flexural fracture properties of the composite mortars with waved-end steel fiber content and the strength class of cement matrix can be a benefit to better interpret the mechanical stability of these composite cementitious mortars [36]. Steel fibers can have a significant beneficial toughening and hardening effect on mortars. In this perspective, an approach aimed at deepening the experimental evaluation of their flexural toughness is required [37]. Furthermore, this approach allows us to evaluate the affordability of this class of steel fibers in order to be suitably applied in plasters.

In such a context, this paper aims to assess the effect on flexural toughening of hooked-end steel fibers in two different classes of cement mortars. In particular, three-point bending tests were performed on FRCM batches differing in terms of fiber weight fractions (0.3, 0.5 and 0.7 wt.%) and cement plaster matrices (M10 and M15). Post-fracture mechanical stability was investigated in terms of strength ratio and toughening indexes for all batches. Besides, a relationship among FRCM microstructure, mechanical behavior and fracture surface was carried out to better recognize the optimal option in terms of mechanical stability and toughness. By expanding our knowledge in these areas, engineers and practitioners can make informed decisions, enabling them to select the most suitable FRCM materials and configurations for specific construction projects. This, in turn, would lead to more resilient and durable reinforced plaster structures, contributing to the overall advancement of construction technology and sustainable building practices.

2 Materials and Methods

2.1 *Materials and sample preparation*

Composite mortars constituted by mixing commercial steel fibers in two cement mortars differing in compressive strength were produced. In particular, M10 and M15 mortars (characterized by a nominal compressive strength of 10 MPa and 15 MPa, respectively) were used as a background plaster. The mortar is supplied by Tradimalt, with the commercial name "Eco-rinforzo" M10 and M15 respectively (Tradimalt, Villafranca (Me), Italy). The two mortars are characterized furthermore by different additives, such as methylcellulose derivative based on nonionic cellulose ether; starch ether especially for dry mixed mortars like adhesives, plasters and trowelling compounds and polycarboxylate powder that combines different mechanisms and is compatible with a variety of cement chemistries.

A single hooked-end steel fiber was added as reinforcement. The metal fiber, namely D3, is a Dramix 3D 80/30GGP (Bekaert, Zwevegem, Belgium) where 80 is the L/D aspect ratio and 30 is referred to the fiber length in mm. A summary of its geometrical and mechanical characteristics is detailed in Table 1.

All mortar formulations were prepared by

Table 1: Properties of the hooked ends steel fiber

	Commercial Code	Dramix 3D 80/30GCP	
D3	Density [kg/dm^3]	1.0	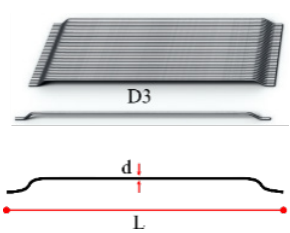
	Diameter, d [mm]	0.38	
	Length, L [mm]	30	
	Aspect ratio	79	
	Elastic modulus [GPa]	200	
	Tensile Strength [MPa]	3070	
	Bundling	Glued	
	Coating	Zinc (galvanized)	

mixing selected binders and aggregates accurately stored under standard conditions (22 °C –60%). The mortars contain the following raw materials: Portlad II/A-LL 42.5 R cement, natural hydraulic lime NHL 5, silica sand (max grain size 2 mm), cellulose ether and starch ether. The mortar constituents were mixed by using a pan mixer.

The water was gradually added (water and mortar ratio 17:100) until the cement slurry was consistent. During mixing, the fibers are added at regular intervals into the mixer to guarantee, during the mixing, a good dispersion of the reinforcement in the mortar. All batches were produced maintaining the same amount of mixing water. The concrete slurry was cast in a metal mold (4 × 4 × 16 cm).

After 2 days, according to EN 1015-11 standard [38], all samples were demolded and stored for 26 days in a humidity and temperature-controlled environment. In particular, FRCM samples at varying fiber content (0.5, 0.7 and 1.0 wt.%) and two cement matrices (M10 and M15) were realized. Details of codes, cement matrix and fiber content for all investigated FRCM batches are reported in Table 2.

Table 2: Codes, cement matrix and fiber content for all investigated FRCM batches

Code	Cement Matrix	Fiber Content [wt.%]
M10	M10	-
M10-D3	M10	0.3
M10-D5	M10	0.5
M10-D7	M10	0.7
M15	M15	--
M15-D3	M15	0.3
M15-D5	M15	0.5
M15-D7	M15	0.7

As references, unreinforced M10 and M15 mortars were prepared. All batches were coded by using an acronym prefix related to the cement matrix class followed by an "-D" letter and number related to the fiber reinforcement content (in wt.%). For example, the M10-D5 batch indicates composite mortar constituted by an M10 matrix and 0.5% of hooked-end steel fibers. The codes M10 and M15 are referred to the unreinforced cement mortars.

As references, unreinforced M10 and M15 mortars were prepared. All batches were coded by using an acronym prefix related to the cement matrix class followed by an "-D" letter and number related to the fiber reinforcement content (in wt.%). For example, the M10-D5 batch indicates composite mortar constituted by an M10 matrix and 0.5 % of hooked-end steel fibers. The codes M10 and M15 are referred to the unreinforced cement mortars.

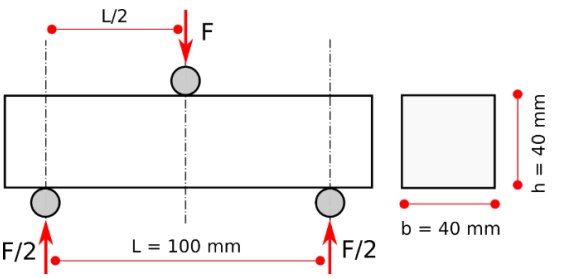

Figure 1: Three-point bending test configuration.

2.2 *Materials characterization*

Three-point load bending (TPB) test has been carried out on prismatic samples (cross-section 40 × 40 mm and length 160 mm) for each mixture by varying the amount of steel fibers. The flexural test was performed on a universal electro-hydraulic testing machine (UTM), Uniframe250 (Controls, Milan, Italy), equipped with a 250 kN load cell. The span length for the three-point bending test was set equal to 100 mm. The three-point bending test configuration is schemed in Figure 1. In order to avoid local displacement mismatch among testing fixtures, a pre-loading of 2 N was applied for all tests. A load-controlled set-up was monotonically applied on the prismatic beam at 10 N/s. All tests were performed in accordance with EN 1015-11 standard. Three replicas for each batch were performed.

3 Results and Discussion

3.1 *Three-point bending test*

shows a reference load versus deflection curve (solid lines in the graph) for a three-point bending test for an unreinforced and hooked-end fiber reinforced M10 mortar ((a) and (b), respectively). Furthermore, in order to better identify the possible development of the damage as the applied load increases, the trend of the slope of the load/displacement curve, identified

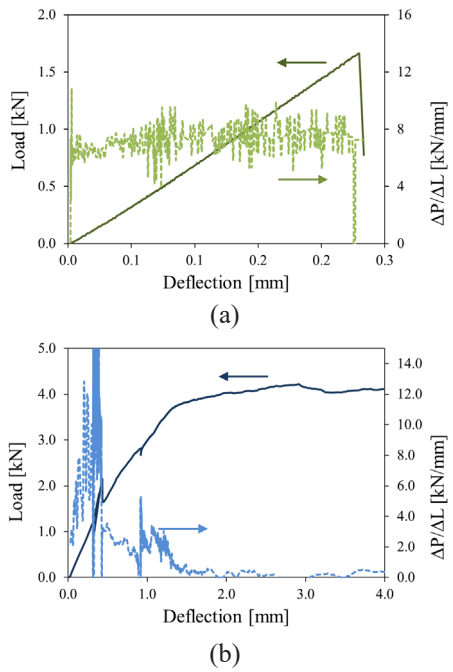

Figure 2: Load (solid line) and ΔP/ΔL (dashed line) vs deflection curves for (a) unreinforced mortar M10 and (b) reinforced mortar M10-D7, under a three-point flexural test.

as ΔP/ΔL is stated for both batches, (dashed lines in).

The unreinforced M10 specimen [(a)] manifests a clear brittle behavior. The trend of the load-displacement curve shows an evident linear elastic behavior until the maximum load is achieved, at ~1.66 kN. Beyond this value, the catastrophic failure of the sample occurs, with a consequent permanent collapse of the post-fracture residual mechanical strength, as experienced by the sudden and without warning fall of the load. These considerations are supported by assessing the ΔP/ΔL trend. This latter, although with a slight random distribution, shows a fairly constant trend at ~7.5 kN/mm, until the maximum load is reached. Beyond this value, the mechanical stability of the sample is compromised and there is a drastic collapse of ΔP/ΔL value.

Different considerations can be drawn by analyzing the trend of the load versus deflection curve for a hooked-end fiber reinforced mortar. In particular as a reference, in (b) the results referred to M10-D7 batch are shown. By evaluating the trend of the curve at low deflection, it is noted that the addition of metal fibers does not involve a significant change in the linear elastic behavior of the mortar. This one can be identified as a pre-cracking stage. The deflection is very low and consequently, the stress state is not sufficient to trigger the formation of cracks or fibers sliding phenomena. This indicates that the cementitious matrix plays a predominant role [39] and the short hooked-end fibers are not able to force relevant change in the mechanical answer of the material. At load ~2.12 kN and a deflection δ of 0.35 mm the matrix cracking takes place. The post-cracking stage of the load vs. deflection curve is, instead, strongly affected by the addition of the short metallic fibers.

Above the threshold load where the matrix cracking occurs, a slight collapse of the load is experienced. In this phase, due to the formation and propagation of stable cracks in the matrix, the post-local-peak behavior was significantly improved by fiber incorporation [40]. Contrasting the unreinforced mortar for which a sudden and catastrophic failure of the specimen was found, in fiber reinforced one a relevant residual mechanical post-cracking strength can be identified. In particular, the composite mortar acquired a deflection-hardening stage. At larger deflection, a gradual recovery of the load can be identified. The load increases monotonically until a maximum load about two times higher than the matrix cracking one (2.13 kN and 4.35 kN, respectively) is obtained. During the deflection-hardening stage, crack formation and propagations are coupled to sliding phenomena at the fiber-matrix interface near the crack, which favors local debonding phenomena [41].

Consequently, the propagation of the crack is strongly hindered by the presence of the reinforcement, which, due to a fiber bridging effect, mainly supplies the applied load [42]. Then, more hooked-end fibers undergo pull-out and the mortar strength decreases. The load gradually decreases at larger deflection, due to the evolution of debonding and pull-out of the residual fibers anchored on the matrix thanks to the hooked-end, identifying a deflection-softening stage.

The damage phenomena due to delamination, debonding and pull-out are largely dissipative energy mechanisms that lead to a significant increase in the strength and deformation at the break of the sample. The fiber reinforced composite mortars did not have a brittle behavior but experienced a relevant residual post-crack resistance. This behavior is ascribed to the hooked-end metal fibers which, offering a bridging effect, act as a structural reinforcement by increasing

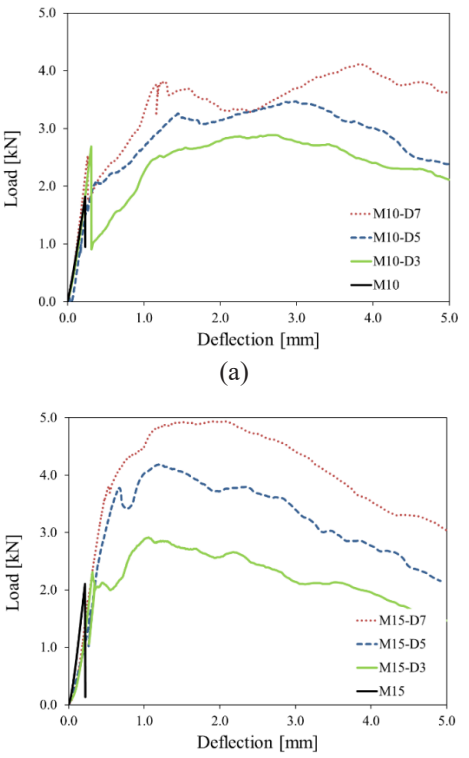

Figure 2: Load (solid line) and ΔP/ΔL (dashed line) vs deflection curves for (a) unreinforced mortar M10 and (b) reinforced mortar M10-D7, under a three-point flexural test.

the energy dissipated during the crack propagation.

With the purpose of better evaluating the effect of the fiber content on the mechanical behavior, under the three-point flexural test, of the fiber reinforced mortars, Figure 3 compares the load vs displacement curves at increasing fiber content for batches constituted by an M10 and M15 matrix (Figure 3(a) and (b), respectively). Generally, the flexural behavior of the FRCM changed radically from brittle to ductile behavior due to the fiber addition. At low deflection, before the first peak, the responses of FRCM are almost similar and linear, suggesting that the flexural behavior in this stage is influenced mainly by the cement matrix properties [39]. At low deflection, the addition of the hooked fibers, even up to 0.7 wt.%, does not have a significant effect on the flexural stiffness of the composite. At the same time, after the first crack, fibers started to suffer the stress by intercepting and bridging the cracks, this hampers the crack propagation and the catastrophic load collapse [43]. In this phase, the metal fibers play an important role in increasing the performance of the residual strength of the composite mortar. This is confirmed, considering that the mechanical stability is greater the higher the fiber content. As a reference, due to the beneficial bridging action of the hooked-end short steel fibers, the maximum strength after the matrix cracking is in the range of about 3000–5000 N and deflection above 2 mm, significantly higher than the unreinforced one.

Moreover, batches with the M15 matrix exhibit better flexural behavior. The use of a high performing cementitious matrix has a positive effect on the hardening and toughening of the matrix. All composite mortars based on the M15 matrix experienced higher strength also a larger deflection than the complementary M10 batches with the same fiber content (the maximum strength of M15 based composites was about 25% higher than M10 based ones). Considering that the M15 plaster is about 6% more expensive (M10 and M15 have a retail price of approx. 36,30€ and 38,50€, respectively) thus opens a new application context where, despite the price, the mechanical performances are an added values (e.g. cultural heritage or anti-seismic restoration). The choice of a more performing matrix contributes to increase the propagation limits of the matrix cracks as well as the required stress to involve the fibers pull-out. Consequently, in M15 based batches, the bridging action is favored thanks to the increase of the crack opening resistance that exalt the interfacial stress transfer efficiency of the FRCM [44]. Consequently, assessment of the load-deflection curves was shown in Figure 3. The improvement in performance due to matrix modification is more relevant in the deflection-hardening and deflection-softening stages than in the deflection at failure. This behavior can be attributed to the improved fiber bridging effect (FBE) that increasing the force required to pull out the fiber contributes positively to stabilize the cracks requiring a higher stress for its propagation [45]. The FBE force is proportional to several factors, such as the fiber–matrix bond and interlocking strength τ_f, the fiber volume fraction V_f and the aspect ratio (l_f/d_f) [46], as in the following Equation (1):

$$\text{FBE} \propto \tau_f V_f (l_f/d_f) \quad (1)$$

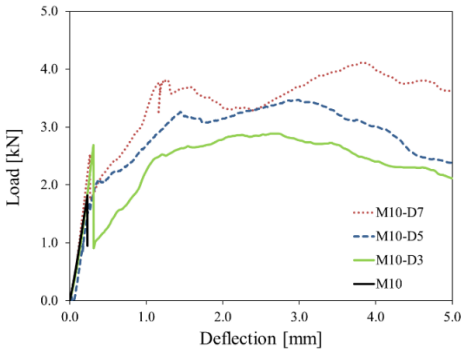

(a)

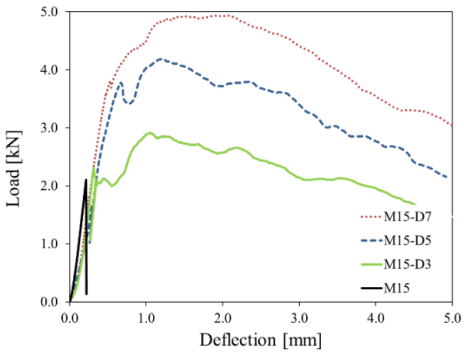

(b)

Figure 3: Load vs deflection curves at increasing fiber content, under three-point flexural test, for (a) composite mortar with M10 matrix (b) composite mortar with M15 matrix.

Where lf and df are the length and diameter of the short fiber, respectively. Considering constant the fiber geometry and volume, the FBE contribution is more relevant as higher is the fiber–matrix interlocking τ_f, [47].

The maximum flexural strength, σ_f, for three-point bending test, can be determined based on the maximum flexural load, Fmax, by Equation (2):

$$\sigma_f = 3F_{max}\, L/(2bh^2) \quad (2)$$

Where b, h and L are the geometrical beam parameters (width, height and span length of the beam, respectively).

Figure 4 compares the maximum flexural strength at increasing fiber content for M10 and M15 based FRCM. In terms of strength, as expected, a progressive improvement of the mortar performances at increasing fiber content is observed. Hence, the increase in flexural

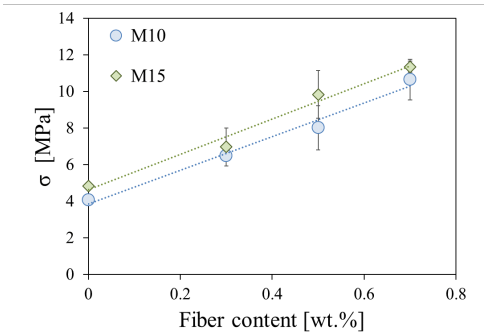

Figure 4: Maximum bending strength at increasing fiber content (solid markers) and correlation line based on mixture rule (dashed line) for M10 and M15 based batches.

strength of M10 batches at increasing fiber content evolved from 4.1 MPa (unreinforced sample, M10) up to the highest value of 10.1 MPa (for M10-D7 batch) with an increase in strength of 146 %. Analogously, for M15 batches, due to hooked-end fiber addition, an increase in strength up to 136% was observed for the M15-D7 batch.

By increasing the amount of the reinforcement, the bridging effect of the hooked-end fibers hinders the crack opening phenomena. The shear strength at the fiber/matrix interface and the high tearing resistance of the terminal hooked side of the fiber allow the reinforcement action of the fiber to be enhanced [48]. Moreover, further considerations can be highlighted by evaluating the correlation between the experimental data and a linear regression fitting (dashed line), referred to estimate the composite mortar strength based on the mixture rule. All batches experienced a good linear correlation at increasing fiber content, thus suggesting that the micro-mechanics mixtures rule could be applied to define with acceptable approximation the trend of the flexural strength. Besides this confirms the good interfacial adhesion and homogeneity of the composite constituents. The specimens with M15 matrix showed slightly higher mechanical strength for all fiber content investigated. However, the trend of the data is clearly comparable (the slope of the fitting line is almost similar). Considering that the composites are constituted by the same type and amount of short steel fibers, it can be deduced that the difference between the two batches could be attributable exclusively to the greater strength of the M15 matrix [49].

Even at low fiber content (0.3 wt.%), the reinforcing action of the fiber is applied. The M10-D3 and M15-D3 batches stated a flexural strength of 6.5 and 7.0 MPa, about 60 and 44% higher than unreinforced ones (M10 and M15 batches, respectively). This behavior is not obvious due to coupled detrimental contributions that could occur in composites at low fiber lengths. In particular, fibers if not well interconnected with the matrix could act as discontinuities despite as reinforcement. This phenomenon is exalted by low adhesion at the fiber-matrix interface or an irregular micro-particle nature of the mortar. The experimental strength value of M10-D3 and M15-D3 is slightly lower than the linear trend line, but always within the error dispersion. It is worth noting that the error dispersion for these batches is slightly greater than the other batches, characterized by a larger fiber content. This behavior could be ascribed to a limited bridging action in the triggering fracture lines during the bending test that is statically influenced by the amount of hooked-end fibers along the fracture line [50].

3.2 *Toughening behavior*

Evaluating the load-deflection curves under three-point bending tests for composite mortars, three main mechanical regimes can be recognized (Figure 5): 1) elastic, 2) deflection-hardening, and 3) defection-softening regimes.

1) Elastic regime. At low deflection, the generated stress and strain are not enough to trigger unstable micro-cracks. The load increases almost linearly at increasing deflection until a first crack in the brittle matrix is generated. When this happens, a sudden collapse of the load occurs and a local maximum of the load can be visualized (PFC, point A).

2) Deflection-hardening regime. At intermediate deflection, after the first-crack activation in the composite mortar matrix, the load gradually increases, indicating a recovery of the mechanical strength. This is defined as deflection-hardening regime. During this phase, the residual load reaches a new local maximum (PDH, point B). This is due to the reinforcing action offered by the hooked-end fibers, which slow down the propagation of the micro-cracks, increasing the load required for their evolution. The cracks, triggered during this phase, grow, and coalesce each other, into a main macro-crack.

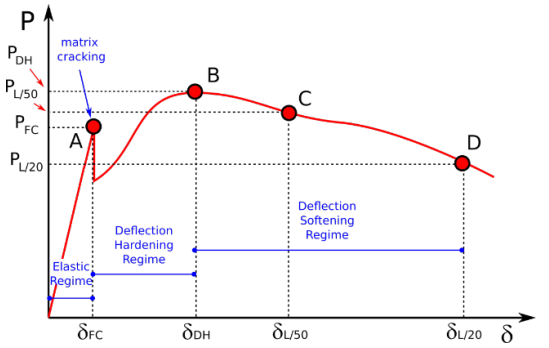

Figure 5: Flexural performance parameters for a compote mortar under three-point bending test.

3) Deflection softening regime. Once the maximum load, marked by point B in the figure, has been exceeded, a progressive reduction in the composite mortar strength at increasing deflection can be found. The mechanical behavior is dominated by a deflection-softening regime. The macro-crack, originating in phase II on the bottom side of the beam, propagates towards the upper internal zone of the beam, leading to a considerable decrease in the resistant section of the sample provoking the reduction of the strength capacity of the sample.

The mechanical hardening and softening regimes play a key role in quantifying the toughening action offered by the fibers to the brittle cementitious matrix. In this concern, with the purpose of better evaluating the toughening contribute supplied by the hooked-end fibers, according to ASTM C1609/C1609M [51], further mechanical features in the load-deflection curve can be defined. In particular, the load values when the deflection is equal to L/50 and L/20 are identified. Considering that L = 100 mm, the threshold deflection is 2 mm (point C) and 5 mm (point D), respectively. Based on points C and D, it is possible to determine the residual load at the net deflection of L/50 and L/20 (PL/50 and PL/20, respectively). Furthermore, TL/50 and TL/20 are the toughness calculated as the area under the load vs. net deflection curve from 0 to L/50 and L/20, respectively.

Table 3 summarizes the main mechanical three-point flexural features of the mortars, acquired from the load-deflection curve, according to Figure 5. In particular, PFC and δFC are the load and deflection of the first crack activation, referred to local peak in point A in Figure 5. Besides, PDH and δDH are the

load and deflection referred to as the maximum peak in the deflection-hardening regime (point B in Figure 5). It is worth noting that more loads (PDH, PL/50 and PL/20) and deflections (δDH) parameters increase at increasing fiber content thanks to the improved load capacity of the hooked-end metal fibers to bear the applied loads. This behavior is related to the crack-bridging action provided by the hooked-end fibers during the crack opening phase and to the increased bearing capacity favored by the interlocking force between the terminal end of the metal fiber and the cement mortar [28]. This trend was not identified for PFC and δFC parameters (point A referred to Figure 5). The δFC does not exhibit a clear dependence from the fiber content in the composite mortar. Considering that PFC and δFC parameters are referred to the activation of crack in the brittle matrix, it is plausible that they are more influenced by the mechanical characteristics of the cement matrix than the fiber content in the composite mortar [52]. As can be seen, by comparing the data relating to batches M10 and M15 in Table 3, the mechanical properties of the mortar, under bending, are affected by the strength and fracture mechanics behavior of the matrix [23].

The load bearing capacity of the metal fibers is influenced by the fiber content cement mortar strength. High fiber content FRCM is characterized by a larger amount of fiber that statically is located in front of the crack tip thus leading to a bridging effect during the crack propagation thus increasing the load bearing capacity [53], [54]. At the same time, a matrix with higher mechanical strength provokes an increase in pull-off strength of hooked-end due to larger force required to remove the interlocked concrete area [49].

The M15-D3 batch experienced a maximum load during the deflection-hardening regime of 2,978 N, about 210 N higher than the M10-D3 one. Analogously, M15-D7 and M10-D7 batches showed a maximum load during the same mechanical regime equal to 4,847 and 4,293 N. These results also confirm that the matrix, similarly to the fiber content, has an important role in the maximum strength of the composite mortar. Furthermore, the slightly greater brittle behavior of the M15 mortar compared to the M10 mortar reveals a much lower deflection value at maximum load for the M15 batches compared to the M10 ones. Furthermore, the dispersion values of δDH are considerably larger for M10 batches, confirming that the trend of their load-deflection curves has a wider plateau during the deflection-hardening and deflection-softening regime with a more indented load evolution during the bending test.

Further information can be acquired by comparing the evolution of the toughness values, TL/50 and TL/20, at increasing fiber content (Figure 6). The toughness was identified in the area under the load vs. deflection curve measured up to a specified L/50 and L/20 deflection, respectively. Considering the brittle behavior of the M10 and M15 mortars, the toughness for fiber content equal to 0% was determined as toughness at fracture for both batches.

The toughness of the FRCM is always higher than the unreinforced mortars. In particular, the M10 mortars reinforced with 0.7 wt.% of metal fibers experienced a TL/50 and TL/20 values about 30 and 90 times higher than the unreinforced ones, respectively. Instead, M15 based FRCM showed slightly lower values of TL/50 and TL/20. In particular, for this FRCM an increase of about 15 and 40 times in the toughness was identified, respectively. This indicates that the M15 FRCM are characterized by TL indices about 2–3 times lower than M15 ones.

Table 3: Flexural loads and deflections for all composite mortars

	Elastic Regime		Deflection-Hardening		Deflection-Softening	
	PFC [N]	**δFC [mm]**	**PDH [N]**	**δDH [mm]**	**PL/50 [N]**	**PL/20 [N]**
M10	1740 ± 108	0.23 ± 0.004	1740 ± 108	0.23 ± 0.004	-	-
M10-D3	2371 ± 240	0.31 ± 0.13	2769 ± 231	1.67 ± 0.974	2355 ± 440	1499 ± 538
M10-D5	2405 ± 195	0.35 ± 0.08	3425 ± 165	2.57 ± 1.280	3217 ± 518	2325 ± 231
M10-D7	2315 ± 167	0.34 ± 0.11	4293 ± 476	3.46 ± 0.654	3926 ± 466	3889 ± 498
M15	2066 ± 60	0.22 ± 0.003	2066 ± 60	0.22 ± 0.003	-	-
M15-D3	2453 ± 181	0.33 ± 0.10	2978 ± 283	1.00 ± 0.333	2316 ± 437	1397 ± 396
M15-D5	3545 ± 213	0.53 ± 0.14	4323 ± 212	1.16 ± 0.203	3884 ± 555	2124 ± 688
M15-D7	3680 ± 184	0.47 ± 0.05	4847 ± 183	1.76 ± 0.158	4170 ± 238	3219 ± 430

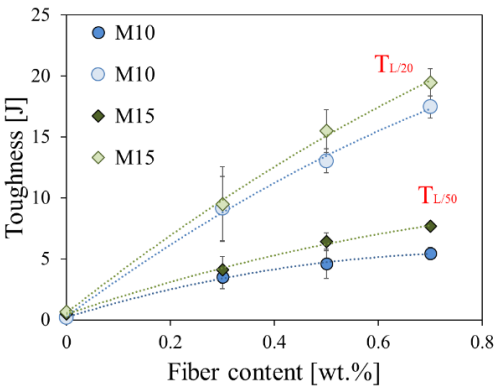

Figure 6: Toughness evolution at increasing fiber content at specified L/50 and L/20 deflection (dark and light-colored markers, respectively) for M10 and M15 mortars (circle and rhombus markers, respectively).

This behavior is mainly due to the load-deflection trend during the deflection-hardening and deflection-softening regime. These regions extend significantly thanks to the presence of the fibers in the mortar. At the same time, the FRCM after the formation of cracks in the matrix suffers a considerably higher load. FRCM characterized by high PL/50 and PL/20 values experienced high toughness values.

In DH and DS regimes, the bending properties of the FRCM are heavily affected by the crack barrier or arrest action supplied by the fibers in the cement matrix [40]. This behavior is also affected by several factors: 1) the amount and shape of the fibers, and 2) strength and stiffness of the matrix [55]. In [55], it was observed that the flexural strength of steel fiber reinforced concrete increased with the concrete age and fiber volume fraction. Therefore, the interlocking action at the hooked-end fiber interface is an important parameter to exalt the post-peak toughness of the mortar. In fact, the pull-off strength of the fiber from the cementitious substrate is influenced by several factors such as the sliding friction, the chemical adhesive force at the fiber/matrix interface, as well as by the mechanical interlocking and the strength of the support [56].

Depending on the geometry of the fiber, one parameter can be preponderant with respect to others. With smooth and straight fibers, the adhesive and sliding friction contributions are the main factors that concur to increase the pull-off resistance. Conversely, for hooked-end fibers, the interlocking contribution is preponderant to offer an increase in the force required to tear the fiber from the support. This interlocking contribution is all the more remarkable the higher the matrix strength. Indeed, as visualized in Figure 6, FRCM batches with the same fiber content, consisting of a more resistant matrix, show greater residual strength of about 20%. Multiple toughening mechanisms cooperate to increase the strength of the fiber-reinforced mortar. The crack shielding mechanism due to the bridging effect acts synergistically with other mechanisms such as activation and propagation of secondary cracks, and containment of the mortar or fiber entanglements [57], [58].

In this concern, with the purpose of better studying the strengthening and toughening contributions supplied by the reinforcement and to better discriminating the post-peak ductility of the FRCM, two indices, strength ratio (SR) and toughness index (TI) were evaluated. In particular, the former [strength ratio, Equation (4)] is defined as the ratio between the equivalent flexural strength, σ_{eq} [Equation (3)], and the first crack strength, σ_{cr}, [59]:

$$\sigma_{eq} = T_k\, L/(bh^2\, \delta_k) \tag{2}$$

$$SR = \sigma_{eq}/\sigma_{cr} \tag{3}$$

where, L, b and h are the span length, width and thickness of the beam, respectively. T_k is the toughness referred to as the k deflection. In this paper, a k equal to L/20 was selected. Moreover, toughness indexes, determined at two k deflections equal to L/50 and L/20 are calculated as [60] [Equations (3) and (6)]:

$$TI_{L/50} = T_{L/50}/T_{FC} \tag{4}$$

$$TI_{L/20} = T_{L/20}/T_{FC} \tag{5}$$

where, $T_{L/50}$ and $T_{L/20}$ are the toughness energy at the L/50 and L/20 deflection, respectively. T_{FC} is the toughness referred to at the first-crack deflection, δ_{FC}. Table 4 summarizes the strength ratio and toughness indexes for all FRCM.

Table 4: Strength ratio and toughness indexes for all FRCM

	σ_{eq} [MPa]	SR	$TI_{L/50}$	$TI_{L/20}$
M10-D3	2.86	0.51	9.5	24.9
M10-D5	4.07	0.72	10.9	31.0
M10-D7	5.45	1.01	13.8	44.2
M15-D3	2.97	0.52	10.0	23.2
M15-D5	4.84	0.58	6.7	16.3
M15-D7	6.09	0.71	8.7	22.1

The SR index increases at increasing hooked-end fiber content, indicating that the load bearing capacity, also a large deflection, is proportional to the fiber content. The strengthening enhancement is due to the hooked-end steel fibers that contribute to stop the crack propagation improving the post-crack mechanical stability [45], [61]. Some differences can be observed in evaluating the TI indexes. Instead, a relevant dependency of the TI index from the cement matrix characteristic can be identified. In particular, despite M10 based batches, for M15 based batches a large amount of fiber content leads to a decrease in the toughening index. This difference is all the more relevant the higher the fiber content. At low fiber content, M15-D3 and M10-D3 batches have a quite similar TI index. Instead M15-D7 batch experienced a TI index about 50% lower than the M10-D7 one. This behavior is attributable to both the high PFC and δFC values and to the progressive reduction of the resistance in correspondence with the maximum load between the DH and DS regimes (PDH) observed for these batches. Consequently, although the energy underlying the load curve is greater, the toughening effect is less pronounced than that found for M10 batches.

3.3 *Fracture morphology*

Figure 7 compares the fracture surface (front and bottom side) of unreinforced and FRCM. As a reference, fractures of M10, M10-D5 and M15-D5 samples were reported. The unreinforced mortar M10 exhibits a brittle and catastrophic fracture. It can be identified only one fracture line that starts from the bottom side of the sample (that suffers the maximum tensile stress) toward the internal zone of the beam longitudinally to the load direction. The low tensile strength of the material is confirmed by the absence of sub-cracks or

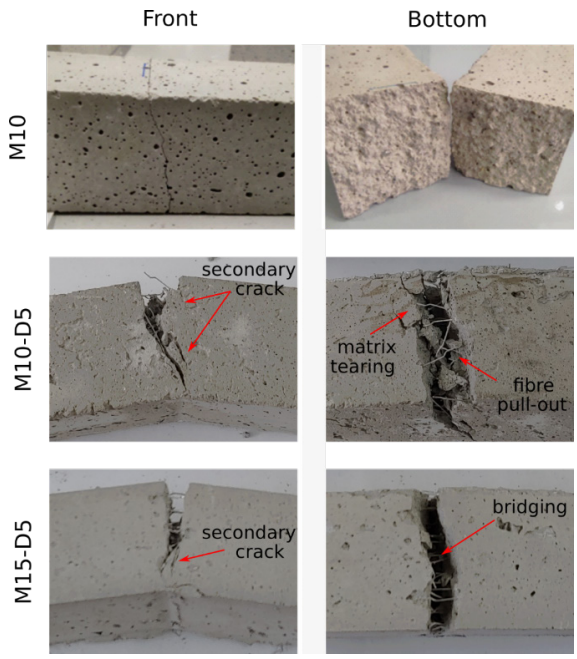

Figure 7: Fracture surfaces of unreinforced mortar (M10) and reinforced M10-D5 and M15-D5 mortars.

secondary energetically dissipative damage phenomena. A similar fracture mechanism, not reported here, was observed for the M15 unreinforced batch.

FRCM shows a more complex fracture evolution. The fracture originates in the matrix on the tension side of the beam (bottom side). Subsequently, the crack propagation evolves progressively in the longitudinal direction to the load. Following the shielding action offered by the metal fibers upon crack opening, the fracture surface is not clear-cut. The FRCM lots show an irregular fracture morphology, with a main crack in the middle of the beam but with several secondary cracks originating from the main one. Indeed, the different mechanisms involved in the damage evolution in the composite beams cause, during the bending test, gradual deviations in the crack's orientation related to the formation and coalescence of secondary cracks close to the main cracks. Therefore, the fracture line is jagged with different areas with matrix tearing or fiber pull-out. Even when the propagation of the main crack approaches the upper side of the beam (near the load application point), the specimen still retains a residual (albeit minimal) load capacity. In this context, Figure 7 depicts the fracture pattern of M10-D5 and M15-D5

batches, which are exemplary of these phenomena. Similar phenomena were also found for the other FRCM batches.

The hooked-end metal fibers offer a beneficial effect on the fracture mechanics of the cement-based mortars, providing a ductile-like bending fracture. Indeed, when the first crack starts, the metal fibers offer a reinforcing contribution thanks to the bridging mechanism, thus stabilizing the crack stress distribution. Then, the crack propagates, and the damaged area increases at increasing displacement. During this phase fiber debonding and pull-out takes place. However, due to the interlocking action of the fiber supplied by the hooked-end geometry large stress values are transferred at the fiber/matrix interface increasing the force required to pull-out the fibers.

Furthermore, this has a key role in triggering secondary fracture mechanisms such as matrix tearing or secondary cracks germination and coalescence. All these concomitant factors increase the dissipative energy contributing to the damage evolution. This is clearly visible in the fracture surface where small portions of cement mortar are locally detached remaining slightly anchored to the main composite structure by the remaining fiber bridges.

The M15 based composite shows a less heterogeneous fracture morphology than the M10 one. This could be attributed to the greater brittle behavior of the M15 matrix compared to the M10 matrix. Furthermore, as evidenced by the load-displacement curves (Figure 3), the M10-based batches show a larger DH and DS region with load fluctuations in a plateau zone. On the other hand, the batches based on M15 experienced, after the PDH load peak, a greater decline in performance. This different mechanical behavior can be found by evaluating that in the M10-based FRCM more degradation mechanisms that contribute to the dissipation of energy during the fracture take place. Conversely, the M15-based batches show a less jagged fracture with a clear phenomenon of main damage at the center line.

Understanding these beneficial effects is essential for optimizing the design and implementation of FRCM in practical applications. The increased flexural strength, combined with enhanced toughness and post-crack resistance, makes these hood-end reinforced composites highly attractive materials for reinforcing and retrofitting various structural elements, contributing to improved structural performance and overall durability. However, further investigations and long-term assessments are still necessary to comprehensively evaluate their behavior under different loading conditions and environmental exposures, ensuring their reliable and efficient use in real-world construction projects.

4 Conclusions

This study investigated the effect of hooked-end steel fiber at varying fiber content (0.3 0.5 and 0.7%) on the toughening behavior of fiber reinforced cement mortars (FRCM) using three-point bending tests. The flexural performance of the FRCM was assessed in terms of strength, deflection and toughness, evidencing that the mechanical bending behavior of the FRCM varies significantly at varying fiber content and cement matrix. The maximum flexural strength observed in the hood-end reinforced composites is significantly higher, reaching about 146 and 134% greater values than the respective unreinforced cement matrix, for M10 and M15 matrices, respectively. These results highlight the substantial improvement in mechanical performance (strengthening and toughening effect) achieved through the addition of hooked-end steel fibers. Moreover, all Fiber-Reinforced Cementitious Mortars (FRCM) displayed a notable strengthening and toughening effect attributed to the inclusion of steel fibers, as evidenced by the toughness index (TI) ranging from 10–45. Among the various combinations studied, the M10-D7 batch, comprising 0.7 wt.% of hooked-end steel fibers in an M10 cement matrix, exhibited the highest TI value, reaching 44. Additionally, unlike the brittle failure observed in unreinforced concrete, all FRCM samples demonstrated a ductile behavior with remarkable residual post-crack resistance, even in composites with relatively low metal fiber content. This remarkable performance can be attributed to the ability of hooked-end fibers to trigger dissipative energy mechanisms, such as internal crack formation and bridging, which significantly extend the post-cracking mechanical stability in terms of residual strength and deflection.

Acknowledgments

This work was supported by the by P.O. FESR Sicilia 2014/2020 (Axis 1, Action 1.1.5 “Support for the

technological advancement of companies through the financing of pilot lines and actions for early validation of products and large-scale demonstrations") Project 082030000276 SMART-ART "Sviluppo di metodi avanzati di restauro, diagnostica e telecontrollo per la conservazione del patrimonio artistico architettonico", CUP G79J18000620007.

Author Contributions

L.C. and F.G.: conceptualization; L.C. and G.G.: methodology; D.P. R.B. and G.G.: validation; L.C.: formal analysis; G.G., P.B. and R.B.: investigation; L.C. and F.G.: resources; L.C., G.G. and D.P.: data curation, L.C.: writing—original draft preparation; G.G., D.P., P.B. and R.B.: writing—review and editing, F.G.: supervision; L.C. and F.G.: funding acquisition; All authors have read and agreed to the published version of the manuscript.

Conflicts of Interest

The authors declare no conflict of interest.

References

[1] A. Habib, R. Begum, and M. M. Alam, "Mechanical properties of synthetic fibers Reinforced Mortars," *International Journal of Scientific and Engineering Research*, vol. 4, no. 4, pp. 923–927, 2013.

[2] A. Bentur and S. Mindess, *Fibre Reinforced Cementitious Composites*. Boca Raton, Florida: CRC Press, 1990.

[3] K. Wille, A. E. Naaman, S. El-Tawil, and G. J. Parra-Montesinos, "Ultra-high performance concrete and fiber reinforced concrete: Achieving strength and ductility without heat curing," *Materials and Structures*, vol. 45, no. 3, pp. 309–324, 2012, doi: 10.1617/s11527-011-9767-0.

[4] E. T. Dawood and M. Ramli, "High strength characteristics of cement mortar reinforced with hybrid fibres," *Construction and Building Materials*, vol. 25, no. 5, pp. 2240–2247, 2011, doi: 10.1016/j.conbuildmat.2010.11.008.

[5] A. M. Brandt, "Fibre reinforced cement-based (FRC) composites after over 40 years of development in building and civil engineering," *Composite Structures*, vol. 86, no. 1, pp. 3–9, 2008, doi: 10.1016/j.compstruct.2008.03.006.

[6] R. B. Jewell, K. C. Mahboub, T. L. Robl, and C. L. Wood, "Influence of cement type on fiber–matrix interface bond strength," *Journal of Materials in Civil Engineering*, vol. 34, no. 4, Apr. 2022, Art. no. 4022003, doi: 10.1061/(ASCE)MT.1943-5533.0004138.

[7] N. Intaboot and K. Chartboot, "Influence and possibility of using limestone dust replacement of sand for sustainability in concrete production," *Applied Science and Engineering Progress*, vol. 15, no. 3, 2022, Art. no. 5575, doi: 10.14416/j.asep.2021.11.002.

[8] S. Jagan, T. R. Neelakantan, and P. Saravanakumar, "Performance enhancement of recycled aggregate concrete - An experimental study," *Applied Science and Engineering Progress*, vol. 15, no. 1, 2022, Art. no. 5212, doi: 10.14416/j.asep.2021.07.003.

[9] C. Subharaj, M. Logesh, A. A. Munaf, J. Srinivas, and S. J. P. Gnanaraj, "Sustainable approach on cement mortar incorporating silica fume, LLDPE and sisal fiber," *Materials Today: Proceedings*, vol. 68, pp. 1342–1348, 2022, doi: 10.1016/j.matpr.2022.06.361.

[10] A. Manoharan and C. Umarani, "Lime mortar, a boon to the environment: Characterization case study and overview," *Sustainability*, vol. 14, no. 11. 2022. doi: 10.3390/su14116481.

[11] M. del Río-Merino, A. Vidales-Barriguete, C. Piña-Ramírez, V. Vitiello, J. S. Cruz-Astorqui, and R. Castelluccio, "A review of the research about gypsum mortars with waste aggregates," *Journal of Building Engineering*, vol. 45, 2022, Art. no. 103338, doi: 10.1016/j.jobe.2021.103338.

[12] H. V. Le, D. Moon, and D. J. Kim, "Effects of ageing and storage conditions on the interfacial bond strength of steel fibers in mortars," *Construction and Building Materials*, vol. 170, pp. 129–141, 2018, doi: 10.1016/j.conbuildmat.2018.03.064.

[13] R. Ralegaonkar, H. Gavali, P. Aswath, and S. Abolmaali, "Application of chopped basalt fibers in reinforced mortar: A review," *Construction and Building Materials*, vol. 164, pp. 589–602, 2018, doi: 10.1016/j.conbuildmat.2017.12.245.

[14] G. Araya-Letelier, P. Maturana, M. Carrasco, F. C. Antico, and M. S. Gómez, "Mechanical-damage

behavior of mortars reinforced with recycled polypropylene fibers," *Sustainability*, vol. 11, no. 8, 2019, doi: 10.3390/su11082200.

[15] M. Małek, M. Jackowski, W. Łasica, M. Kadela, and M. Wachowski, "Mechanical and material properties of mortar reinforced with glass fiber: An experimental study," *Materials*, vol. 14, no. 3. 2021, doi: 10.3390/ma14030698.

[16] A. Belli, A. Mobili, T. Bellezze, and F. Tittarelli, "Commercial and recycled carbon/steel fibers for fiber-reinforced cement mortars with high electrical conductivity," *Cement and Concrete Composites*, vol. 109, 2020, Art. no. 103569, doi: 10.1016/j.cemconcomp.2020.103569.

[17] M. Cao, Z. Liu, and C. Xie, "Effect of steel-PVA hybrid fibers on compressive behavior of $CaCO_3$ whiskers reinforced cement mortar," *Journal of Building Engineering*, vol. 31, 2020, Art. no. 101314, doi: 10.1016/j.jobe.2020.101314.

[18] F. Koksal, M. S. Yıldırım, A. Benli, and O. Gencel, "Hybrid effect of micro-steel and basalt fibers on physico-mechanical properties and durability of mortars with silica fume," *Case Studies in Construction Materials*, vol. 15, 2021, Art. no. e00649, doi: 10.1016/j.cscm.2021.e00649.

[19] A. Suwansaard, T. Kongpun, and M. Khemkhao, "Properties of mortars mixed with polystyrene and hemp fiber wastes," *Applied Science and Engineering Progress*, vol. 15, no. 1, 2022, Art. no. 5405, doi: 10.14416/j.asep.2021.09.004.

[20] D. Wang, C. Shi, Z. Wu, J. Xiao, Z. Huang, and Z. Fang, "A review on ultra high performance concrete: Part II. Hydration, microstructure and properties," *Construction and Building Materials*, vol. 96, pp. 368–377, 2015, doi: 10.1016/j.conbuildmat.2015.08.095.

[21] S. T. Kang, B. Y. Lee, J.-K. Kim, and Y. Y. Kim, "The effect of fibre distribution characteristics on the flexural strength of steel fibre-reinforced ultra high strength concrete," *Construction and Building Materials*, vol. 25, no. 5, pp. 2450–2457, 2011, doi: 10.1016/j.conbuildmat.2010.11.057.

[22] A. M. Rashad, "Effect of steel fibers on geopolymer properties – The best synopsis for civil engineer," *Construction and Building Materials*, vol. 246, 2020, Art. no. 118534, doi: 10.1016/j.conbuildmat.2020.118534.

[23] D.-Y. Yoo, S.-W. Kim, and J.-J. Park, "Comparative flexural behavior of ultra-high-performance concrete reinforced with hybrid straight steel fibers," *Construction and Building Materials*, vol. 132, pp. 219–229, 2017, doi: 10.1016/j.conbuildmat.2016.11.104.

[24] B. Figiela, H. Šimonová, and K. Korniejenko, "State of the art, challenges, and emerging trends: Geopolymer composite reinforced by dispersed steel fibers," *Reviews on Advanced Materials Science*, vol. 61, no. 1, pp. 1–15, 2022, doi: 10.1515/rams-2021-0067.

[25] M. A. Faris, M. M. A. B. Abdullah, R. Muniandy, M. F. A. Hashim, K. Błoch, B. Jeż, S. Garus, P. Palutkiewicz, N. A. M. Mortar, and M. F. Ghazali, "Comparison of Hook and straight steel fibers addition on malaysian fly ash-based geopolymer concrete on the slump, density, water absorption and mechanical properties," *Materials*, vol. 14, no. 5, 2021, doi: 10.3390/ma14051310.

[26] X. Zheng, J. Zhang, and Z. Wang, "Effect of multiple matrix cracking on crack bridging of fiber reinforced engineered cementitious composite," *Journal of Composite Materials*, vol. 54, no. 26, pp. 3949–3965, May 2020, doi: 10.1177/0021998320923145.

[27] A. Abushanab, W. Alnahhal, M. G. Sohail, N. Alnuaimi, R. Kahraman, and N. Altayeh, "Mechanical and durability properties of ultra-high performance steel FRC made with discarded materials," *Journal of Building Engineering*, vol. 44, 2021, Art. no. 103264, doi: 10.1016/j.jobe.2021.103264.

[28] Z. Wu, C. Shi, W. He, and L. Wu, "Effects of steel fiber content and shape on mechanical properties of ultra high performance concrete," *Construction and Building Materials*, vol. 103, pp. 8–14, 2016, doi: 10.1016/j.conbuildmat.2015.11.028.

[29] Y. Zhang, J. W. Ju, Q. Chen, Z. Yan, H. Zhu, and Z. Jiang, "Characterizing and analyzing the residual interfacial behavior of steel fibers embedded into cement-based matrices after exposure to high temperatures," *Composites Part B: Engineering*, vol. 191, 2020, Art. no. 107933, doi: 10.1016/j.compositesb.2020.107933.

[30] G. Ruano, F. Isla, B. Luccioni, R. Zerbino, and G. Giaccio, "Steel fibers pull-out after exposure to high temperatures and its contribution to the

residual mechanical behavior of high strength concrete," *Construction and Building Materials*, vol. 163, pp. 571–585, 2018, doi: 10.1016/j.conbuildmat.2017.12.129.

[31] C. Fang, M. Ali, T. Xie, P. Visintin, and A. H. Sheikh, "The influence of steel fibre properties on the shrinkage of ultra-high performance fibre reinforced concrete," *Construction and Building Materials*, vol. 242, 2020, Art. no. 117993, doi: 10.1016/j.conbuildmat.2019.117993.

[32] X. Ding, M. Zhao, H. Li, Y. Zhang, Y. Liu, and S. Zhao, "Bond behaviors of steel fiber in mortar affected by inclination angle and fiber spacing," *Materials*, vol. 15, no. 17, 2022, doi: 10.3390/ma15176024.

[33] F. Sulthan and Saloma, "Influence of hooked-endsteel fibers on fresh and hardened properties of steel fiber reinforcement self-compacting concrete (SFRSCC)," *Journal of Physics: Conference Series*, vol. 1198, no. 3, 2019, Art. no. 32005, doi: 10.1088/1742-6596/1198/3/032005.

[34] L. Kheddache, K. Chahour, and B. Safi, "Effect of fiber distribution on the mechanical behavior in bending of self-compacting mortars," *Selected Scientific Papers - Journal of Civil Engineering*, vol. 15, no. 1, pp. 129–148, 2020, doi: 10.1515/sspjce-2020-0012.

[35] L. Kheddache, C. Aribi, K. Chahour, and B. Safi, "Highlighting of the distribution effect of steel hook fibers at low and high dosage on the flexural strength of self-compacting mortars," *Materials Today: Proceedings*, vol. 52, pp. 1384–1390, 2022, doi: 10.1016/j.matpr.2021.11.125.

[36] S. Khan, L. Qing, I. Ahmad, R. Mu, and M. Bi, "Investigation on fracture behavior of cementitious composites reinforced with aligned hooked-end steel fibers," *Materials*, vol. 15, no. 2. 2022, doi: 10.3390/ma15020542.

[37] Y. Zhang, S. Li, T. Zhu, and G. Li, "Numerical analysis of bending toughness of steel fiber reinforced cement based materials," *Highlights in Science, Engineering and Technology*, vol. 51, pp. 217–225, 2023, doi: 10.54097/hset.v51i.8269.

[38] *Methods of test for mortar for masonry Determination of flexural and compressive strength of hardened mortar*, Standard EN 1015-11, 2019.

[39] M. Sappakittipakorn, P. Sukontasukkul, H. Higashiyama, and P. Chindaprasirt, "Properties of hooked end steel fiber reinforced acrylic modified concrete," *Construction and Building Materials*, vol. 186, pp. 1247–1255, 2018, doi: 10.1016/j.conbuildmat.2018.08.055.

[40] Y. Ding and Y.-L. Bai, "Fracture properties and softening curves of steel fiber-reinforced slag-based geopolymer mortar and concrete," *Materials*, vol. 11, no. 8, 2018, doi: 10.3390/ma11081445.

[41] D. Zhang, Y. Ge, S. D. Pang, and P. Liu, "The effect of fly ash content on flexural performance and fiber failure mechanism of lightweight deflection-hardening cementitious composites," *Construction and Building Materials*, vol. 302, 2021, Art. no. 124349, doi: 10.1016/j.conbuildmat.2021.124349.

[42] A. Venkateshwaran, K. H. Tan, and Y. Li, "Residual flexural strengths of steel fiber reinforced concrete with multiple hooked-end fibers," *Structural Concrete*, vol. 19, no. 2, pp. 352–365, Apr. 2018, doi: 10.1002/suco.201700030.

[43] C. Redon and J.-L. Chermant, "Compactness of the cement microstructure versus crack bridging in mortars reinforced with amorphous cast iron fibers and silica fumes," *Applied Composite Materials*, vol. 8, no. 3, pp. 149–161, 2001, doi: 10.1023/A:1011245515368.

[44] M. Kheradmand, M. Mastali, Z. Abdollahnejad, and F. Pacheco-Torgal, "Experimental and numerical investigations on the flexural performance of geopolymers reinforced with short hybrid polymeric fibres," *Composites Part B: Engineering*, vol. 126, pp. 108–118, 2017, doi: 10.1016/j.compositesb.2017.06.001.

[45] S. Abdallah, M. Fan, and X. Zhou, "Pull-out behaviour of hooked end steel fibres embedded in ultra-high performance mortar with various W/B ratios," *International Journal of Concrete Structures and Materials*, vol. 11, no. 2, pp. 301–313, 2017, doi: 10.1007/s40069-017-0193-8.

[46] F. Aslani and S. Nejadi, "Bond characteristics of steel fiber and deformed reinforcing steel bar embedded in steel fiber reinforced self-compacting concrete (SFRSCC)," *Central European Journal of Engineering*, vol. 2, no. 3, pp. 445–470, 2012, doi: 10.2478/s13531-012-0015-3.

[47] L. Huang, Y. Chi, L. Xu, P. Chen, and A. Zhang,

"Local bond performance of rebar embedded in steel-polypropylene hybrid fiber reinforced concrete under monotonic and cyclic loading," *Construction and Building Materials*, vol. 103, pp. 77–92, 2016, doi: 10.1016/j.conbuildmat.2015.11.040.

[48] S. Abdallah and D. W. A. Rees, "Comparisons between pull-out behaviour of various hooked-end fibres in normal–high strength concretes," *International Journal of Concrete Structures and Materials*, vol. 13, no. 1, p. 27, 2019, doi: 10.1186/s40069-019-0337-0.

[49] T. Abu-Lebdeh, S. Hamoush, W. Heard, and B. Zornig, "Effect of matrix strength on pullout behavior of steel fiber reinforced very-high strength concrete composites," *Construction and Building Materials*, vol. 25, no. 1, pp. 39–46, 2011, doi: 10.1016/j.conbuildmat.2010.06.059.

[50] C. A. O. Okeh, D. W. Begg, S. J. Barnett, and N. Nanos, "Behaviour of hybrid steel fibre reinforced self compacting concrete using innovative hooked-end steel fibres under tensile stress," *Construction and Building Materials*, vol. 202, pp. 753–761, 2019, doi: 10.1016/j.conbuildmat.2018.12.067.

[51] *A Standard Test Method for Flexural Performance of Fiber-Reinforced Concrete (Using Beam With Third-Point Loading)*. STM C1609/C1609M-12, 2012. [Online]. Available: https://www.astm.org/c1609_c1609m-12.html

[52] Ş. Yazıcı, G. İnan, and V. Tabak, "Effect of aspect ratio and volume fraction of steel fiber on the mechanical properties of SFRC," *Construction and Building Materials*, vol. 21, no. 6, pp. 1250–1253, 2007, doi: 10.1016/j.conbuildmat.2006.05.025.

[53] R. Hameed, A. Turatsinze, F. Duprat, and A. Sellier, "Metallic fiber reinforced concrete: Effect of fiber aspect ratio on the flexural properties," *Journal of Engineering and Applied Sciences*, vol. 4, no. 5, pp. 67–72, 2009.

[54] W. Abbass, M. I. Khan, and S. Mourad, "Evaluation of mechanical properties of steel fiber reinforced concrete with different strengths of concrete," *Construction and Building Materials*, vol. 168, pp. 556–569, 2018, doi: 10.1016/j.conbuildmat.2018.02.164.

[55] T. Uygunoğlu, "Investigation of microstructure and flexural behavior of steel-fiber reinforced concrete," *Materials and Structures*, vol. 41, no. 8, pp. 1441–1449, 2008, doi: 10.1617/s11527-007-9341-y.

[56] E. Zīle and O. Zīle, "Effect of the fiber geometry on the pullout response of mechanically deformed steel fibers," *Cement and Concrete Research*, vol. 44, pp. 18–24, 2013, doi: 10.1016/j.cemconres.2012.10.014.

[57] S. Das, M. H. R. Sobuz, V. W. Y. Tam, A. S. M. Akid, N. M. Sutan, and F. M. M. Rahman, "Effects of incorporating hybrid fibres on rheological and mechanical properties of fibre reinforced concrete," *Construction and Building Materials*, vol. 262, 2020, Art. no. 120561, doi: 10.1016/j.conbuildmat.2020.120561.

[58] A. Bentur, S. Mindess, and S. Diamond, "Pull-out processes in steel fibre reinforced cement," *International Journal of Cement Composites and Lightweight Concrete*, vol. 7, no. 1, pp. 29–37, 1985, doi: 10.1016/0262-5075(85)90024-7.

[59] B. Li, Y. Chi, L. Xu, Y. Shi, and C. Li, "Experimental investigation on the flexural behavior of steel-polypropylene hybrid fiber reinforced concrete," *Construction and Building Materials*, vol. 191, pp. 80–94, 2018, doi: 10.1016/j.conbuildmat.2018.09.202.

[60] P. S. Song and S. Hwang, "Mechanical properties of high-strength steel fiber-reinforced concrete," *Construction and Building Materials*, vol. 18, no. 9, pp. 669–673, 2004, doi: 10.1016/j.conbuildmat.2004.04.027.

[61] X. Ding, H. Geng, M. Zhao, Z. Chen, and J. Li, "Synergistic bond properties of different deformed steel fibers embedded in mortars wet-sieved from self-compacting SFRC," *Applied Sciences*, vol. 11, no. 21, 2021, Art. no. 10144, doi: 10.3390/app112110144.